Electron Interferometry and EELS

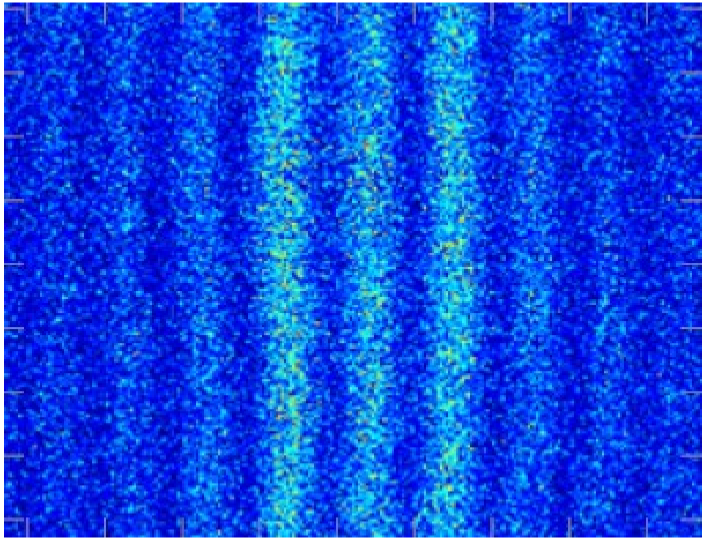

M&M 2026
MICROSCOPY &
MICROANALYSIS
August 2-6 • Milwaukee, WI

Dr. David Kordahl

Centenary
COLLEGE OF LOUISIANA

Outline

- Review of electron interferometry experiments
- Examine the logical structure of calculations
- Connect calculations to standard EELS models
- Explore possible “next step” experiments

Fringe Contrast and “Visibility”

- Conceptually, easy to understand how “fringe visibility” is found from an inteferogram
- Variation between min and max gives us the visibility

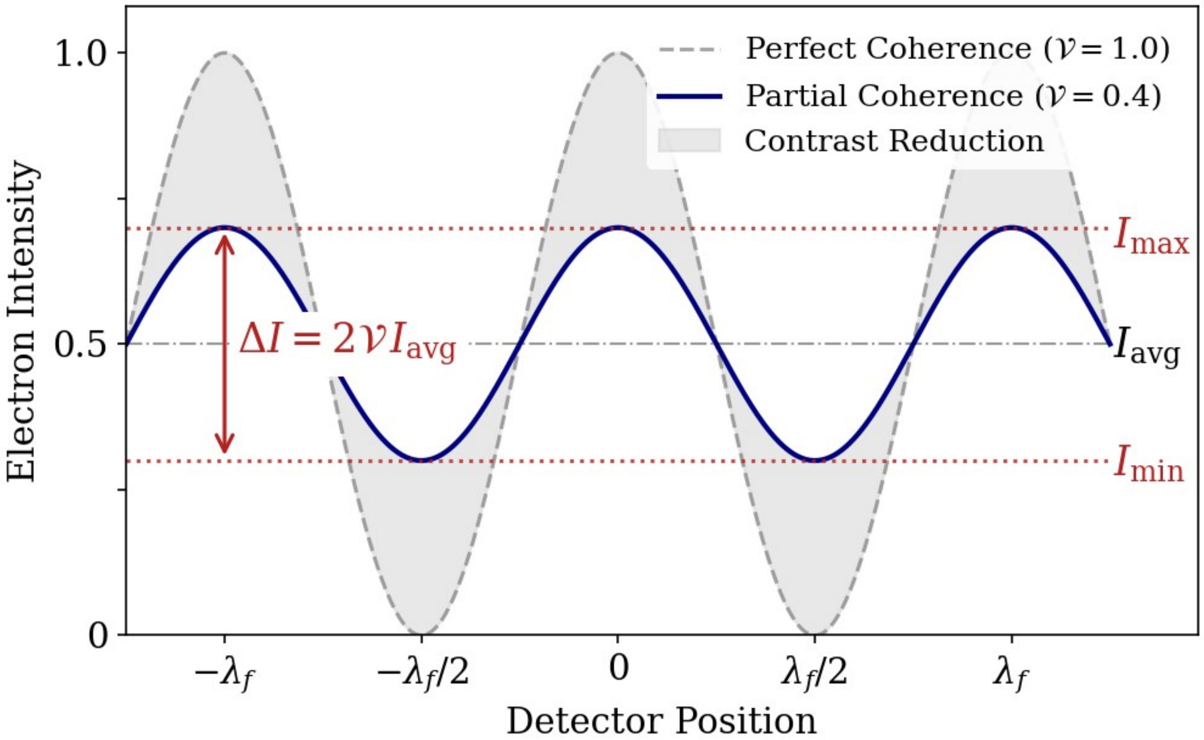

$$\Delta I = I_{max} - I_{min} = 2\mathcal{V} I_{avg}$$

- Limits: $V = 1 \rightarrow$ max contrast
  $V = 0 \rightarrow$ min contrast

Experiments in Fringe Visibility

- Empirical observation: fringe visibility decreases as the electron
  - Passes nearer to the dielectric surface
  - Has farther separated paths

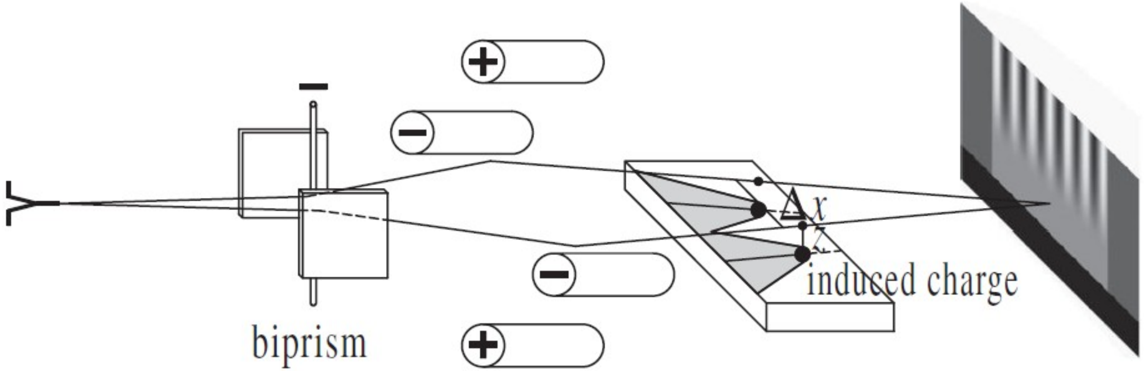

"Measurement of Decoherence of Electron Waves and Visualization of the Quantum-Classical Transition," Peter Sonnentag and Franz Hasselbach, *Physical Review Letters* 98, 200402 (2007)

Experiments in Fringe Visibility

- Empirical observation: fringe visibility decreases as the electron
  - Passes nearer to the dielectric surface
  - Has farther separated paths

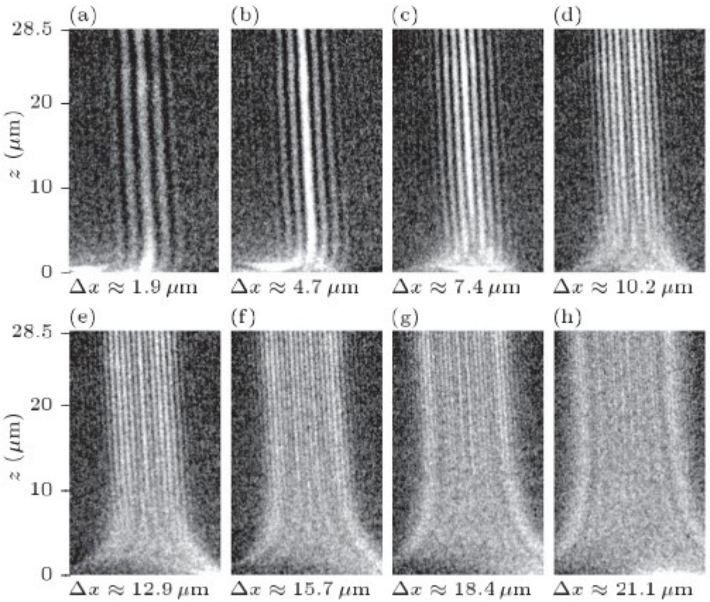

"Measurement of Decoherence of Electron Waves and Visualization of the Quantum-Classical Transition," Peter Sonnentag and Franz Hasselbach, *Physical Review Letters* 98, 200402 (2007)

Experiments in Fringe Visibility

- Empirical observation: fringe visibility decreases as the electron
  - Passes nearer to the dielectric surface
  - Has farther separated paths

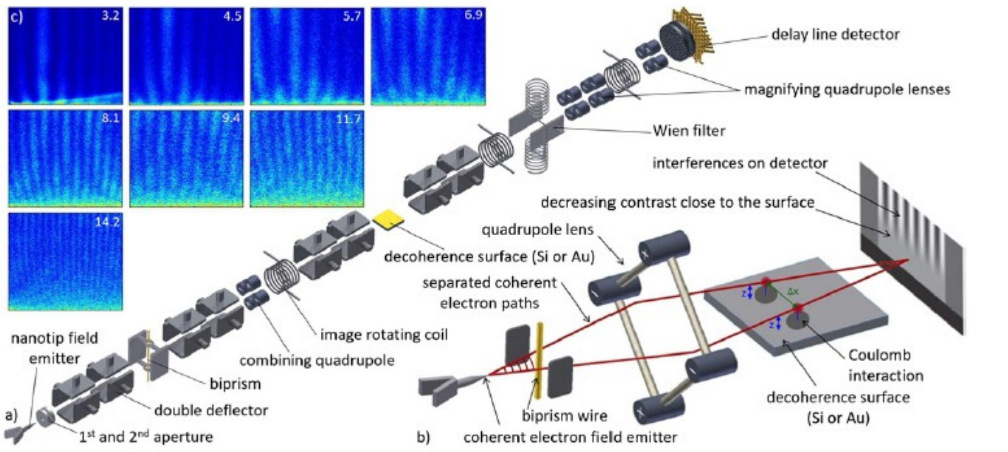

Figure 1. (a) Experimental setup for electron decoherence measurements close to a semiconducting and metallic environment. (b) Sketch of the experiment, where a coherent electron beam is separated and combined by an electrostatic biprism and a quadrupole lens. In the quantum superposition state before interference, the beam passes aloof a semiconducting n-doped silicon or gold surface, interacting with the bulk electron gas. This process causes decoherence which can be observed in a decreasing interference contrast close to the surface. (c) Recorded fringe pattern above the silicon surface (bottom edge of each image) for different beam path separations Δx (value in upper right corner in μm). The top edge is at a height $z = 40$ μm. An increase in signal above the surface up to max 4 μm is visible that is assumed to be due to scattering on waver edge defects.

"Quantum decoherence by Coulomb interaction,"
N. Kerker, R. Röpke, L.M. Steinert, A. Pooch, and A. Stibor,
New Journal of Physics 22 (2020) 0630391

Experiments in Fringe Visibility

- Kerker *et al.* (2020) tested various models of visibility predicted from entanglement of electron and plate

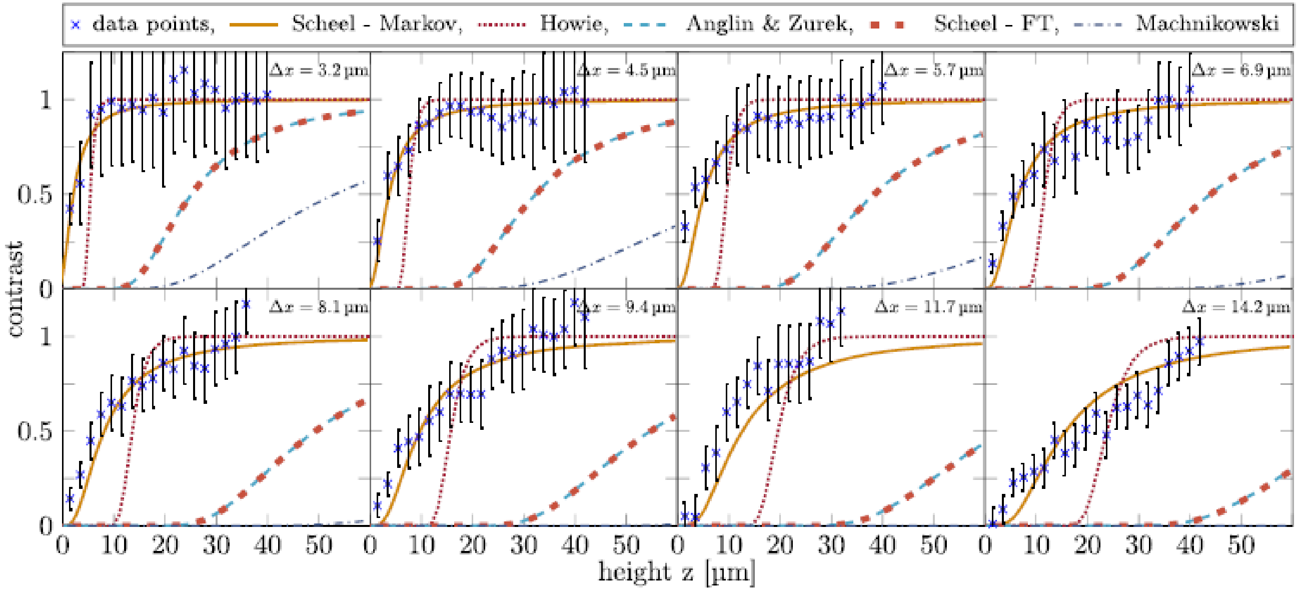

Figure 2. Decoherence of electrons in a superposition state close to a doped silicon surface. The loss of visibility is plotted as a function of distance z to the semiconducting plate for different beam path separations Δx and compared to four current theoretical models [5–8].

Experiments in Fringe Visibility

- Kerker *et al.* (2020) tested various models of visibility predicted from entanglement of electron and plate
- The "Scheel-Markov" theory is basically successful; how does it relate to EELS models?

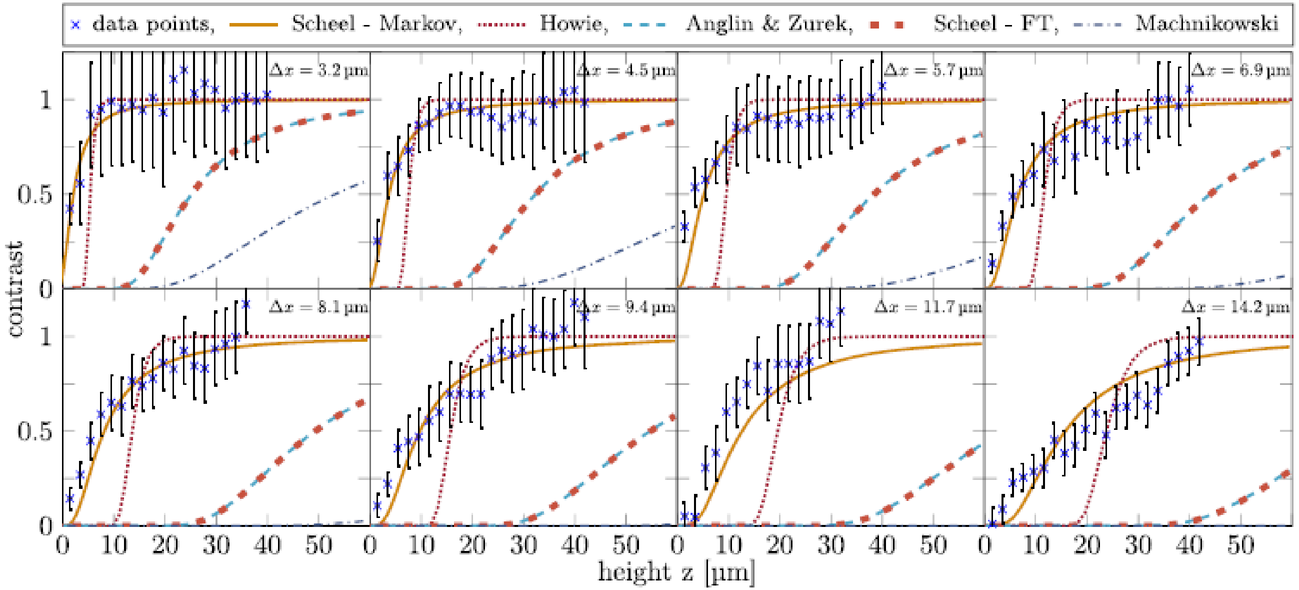

Figure 2. Decoherence of electrons in a superposition state close to a doped silicon surface. The loss of visibility is plotted as a function of distance z to the semiconducting plate for different beam path separations Δx and compared to four current theoretical models [5–8].

Howie's Idea: EELS → Visibility

- Decoherence rate sums EEL spectrum for modes that interact with the different paths differently
  ($d < \lambda$, or $|k| > \alpha/d$)

"Mechanisms of decoherence in electron microscopy," Archie Howie, *Ultramicroscopy* 111 (2011) 761–767.

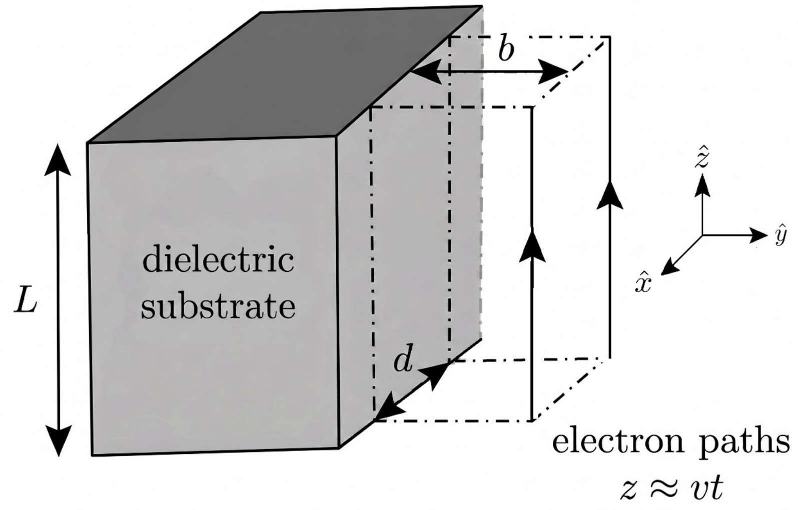

Howie’s Idea: EELS → Visibility

- Decoherence rate sums EEL spectrum for modes that interact with the different paths differently
(d < λ, or |k| > α/d)

$$\gamma(b,d,T) = \int_0^\infty \mathrm{d}\omega \int_{\alpha/d}^\infty \mathrm{d}k_x \, \frac{\mathrm{d}^3 P}{\mathrm{d}\omega \, \mathrm{d}k_x \, \mathrm{d}z} \coth\left(\frac{\hbar\omega}{2k_B T}\right) + \int_0^\infty \mathrm{d}\omega \int_{-\infty}^{-\alpha/d} \mathrm{d}k_x \, \frac{\mathrm{d}^3 P}{\mathrm{d}\omega \, \mathrm{d}k_x \, \mathrm{d}z} \coth\left(\frac{\hbar\omega}{2k_B T}\right)$$

$$\mathcal{V} = \mathrm{e}^{-\gamma(b,d,T)L}$$

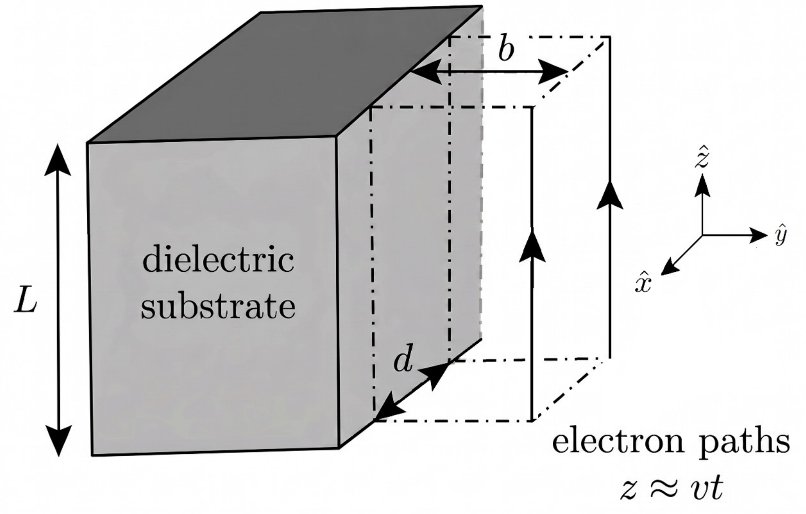

“Mechanisms of decoherence in electron microscopy,” Archie Howie, *Ultramicroscopy* 111 (2011) 761–767.

Howie's Idea: EELS → Visibility

- Decoherence rate sums EEL spectrum for modes that interact with the different paths differently
  ($d < \lambda$, or $|k| > \alpha/d$)

$$\gamma(b,d,T) = \int_0^\infty \mathrm{d}\omega \int_{\alpha/d}^{\infty} \mathrm{d}k_x \, \frac{\mathrm{d}^3 P}{\mathrm{d}\omega\, \mathrm{d}k_x\, \mathrm{d}z} \coth\left(\frac{\hbar\omega}{2k_B T}\right) + \int_0^\infty \mathrm{d}\omega \int_{-\infty}^{-\alpha/d} \mathrm{d}k_x \, \frac{\mathrm{d}^3 P}{\mathrm{d}\omega\, \mathrm{d}k_x\, \mathrm{d}z} \coth\left(\frac{\hbar\omega}{2k_B T}\right)$$

$$\mathcal{V} = \mathrm{e}^{-\gamma(b,d,T)L}$$

"Mechanisms of decoherence in electron microscopy," Archie Howie, *Ultramicroscopy* 111 (2011) 761–767.

Right scale… can we fix this idea?

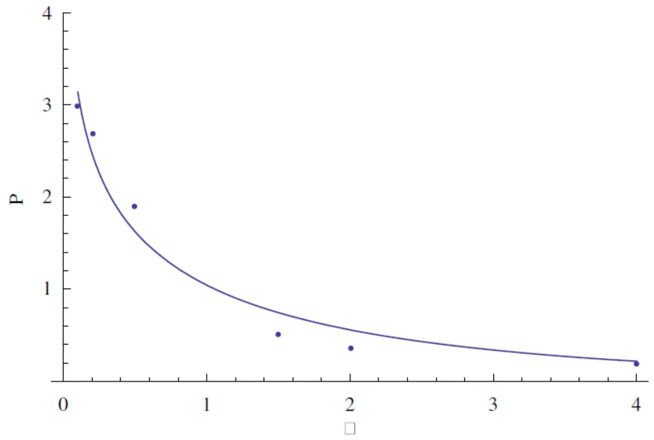

Fig. 4. Comparison between points for $P=-\ln(V)$, where V is the measured fringe visibility in aloof beam electron holography [19] and the theory of Eq. (7) represented by the function $E_1(\eta)$, where $\eta=4x_0/\Delta y$.

Pedagogical Model of Fringe Visibility

- Back to basics: 1D quantum model
- x = coordinate of propagating electron
- X = coordinate of proton in slit
- Probability of observing electron at position x on screen:

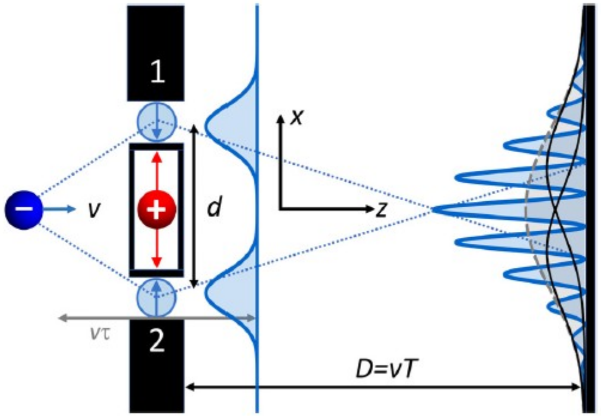

$$P_e(x) = \int_{-\infty}^{\infty} |\Psi_{out}(x, X)|^2 dX.$$

Decoherence, entanglement, and information in the electron double-slit experiment with monitoring

https://doi.org/10.1119/5.0210117

Frederick W. Strauch[a)]

Pedagogical Model of Fringe Visibility

- In Strauch's 1D model, "which path" information is encoded as a phase factors to conserve momentum

$$\Psi_{\text{in}}(x,X) = \frac{1}{\sqrt{2}}\psi_1(x)\psi_{\text{p}}(X) + \frac{1}{\sqrt{2}}\psi_2(x)\psi_{\text{p}}(X) \longrightarrow \Psi_{\text{out}}(x,X) = \frac{1}{\sqrt{2}}\psi_1(x)e^{-iPx/\hbar}\psi_{\text{p}}(X)e^{+iPX/\hbar} + \frac{1}{\sqrt{2}}\psi_2(x)e^{+iPx/\hbar}\psi_{\text{p}}(X)e^{-iPX/\hbar}.$$

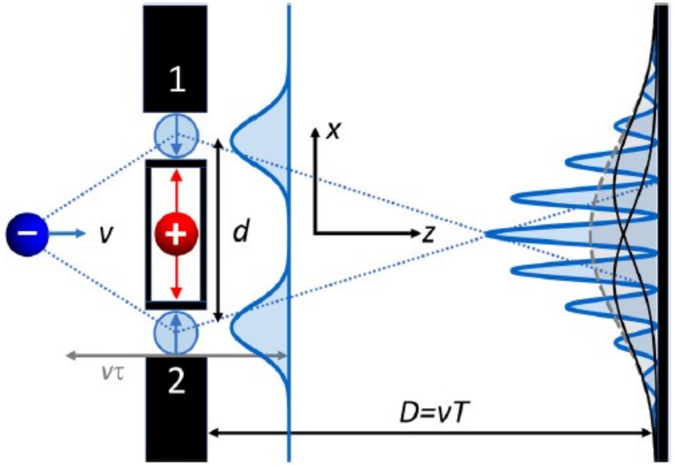

$$\frac{1}{\sqrt{2}}|\text{“electron in slit 1”}\rangle|\text{“proton moving up”}\rangle + \frac{1}{\sqrt{2}}|\text{“electron in slit 2”}\rangle|\text{“proton moving down”}\rangle.$$

Pedagogical Model of Fringe Visibility

- Summing over proton states smears out the observable electron fringes: $P_e(x) = \int_{-\infty}^{\infty} |\Psi_{out}(x, X)|^2 dX.$
- Visibility reduction correlates with interaction

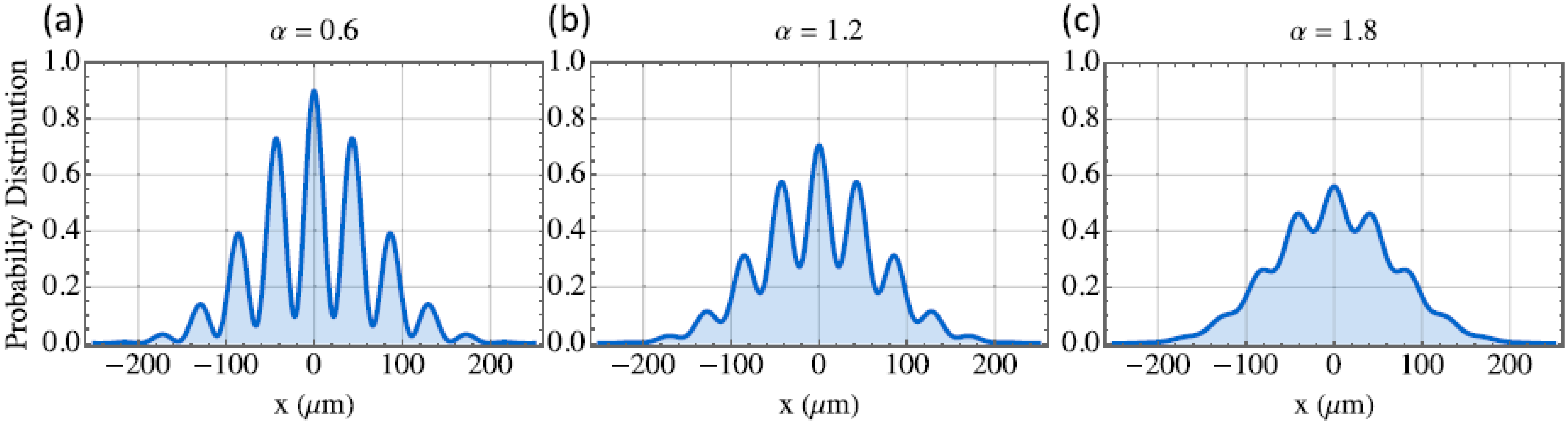

Increasing interaction strength
Decreasing fringe visibility

3D Version of the Interaction Model

- Experimental situation is nearly the same as Strauch, but "which path" information depends on *L*, *d*, and *b*
- Before interaction, assume the substrate is in its ground state, and the electron is in a split-path

$$|\Psi_e\rangle = \frac{1}{\sqrt{2}}\left[\psi_{\mathrm{R}}(\mathbf{x}_\perp) + \psi_{\mathrm{L}}(\mathbf{x}_\perp)\right]$$

$$|\Psi_i\rangle = |\Psi_e\rangle \otimes |0\rangle$$

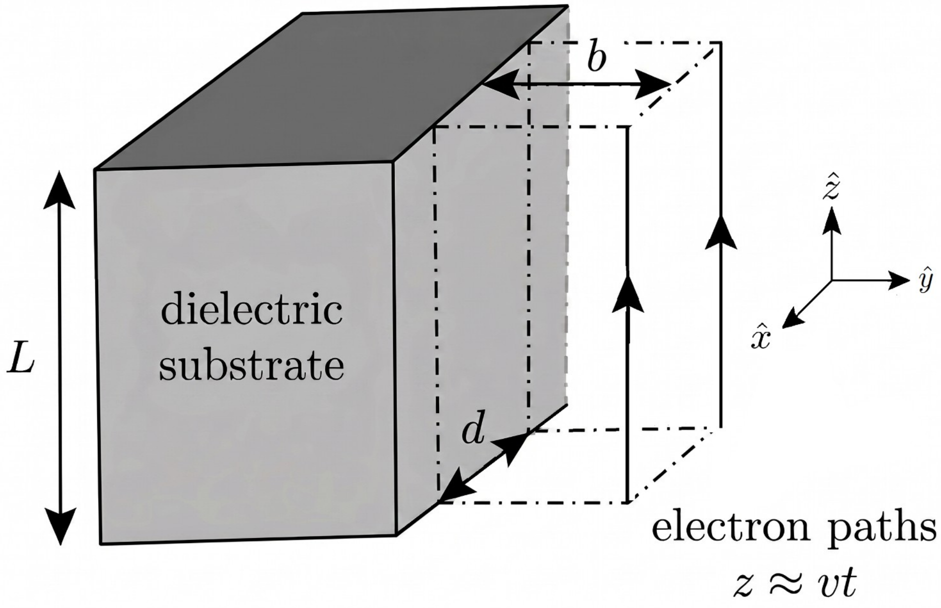

3D Version of the Interaction Model

- Keeping first-order excitations of surface modes with wavevector **k**, the wavefunction after interaction is

$$|\Psi_f\rangle = \frac{1}{\sqrt{2}}\Bigg[\psi_{\rm R}(\mathbf{x}_\perp)\left(c_{\rm R0}\,|0\rangle + \sum_{\mathbf{k}} c_{\rm R\mathbf{k}}\,|1_{\mathbf{k}}\rangle\right) + \psi_{\rm L}(\mathbf{x}_\perp)\left(c_{\rm L0}\,|0\rangle + \sum_{\mathbf{k}} c_{\rm L\mathbf{k}}\,|1_{\mathbf{k}}\rangle\right)\Bigg]$$

- Afterward, the wave packets are made to overlap, and we sum over surface modes:

$$P_e(\mathbf{x}_\perp) = \sum_{\{n_{\mathbf{k}}\}} \langle\Psi_f|\mathbb{I}_{\rm el}\otimes|\{n_{\mathbf{k}}\}\rangle\,\langle\{n_{\mathbf{k}}\}|\,|\Psi_f\rangle$$

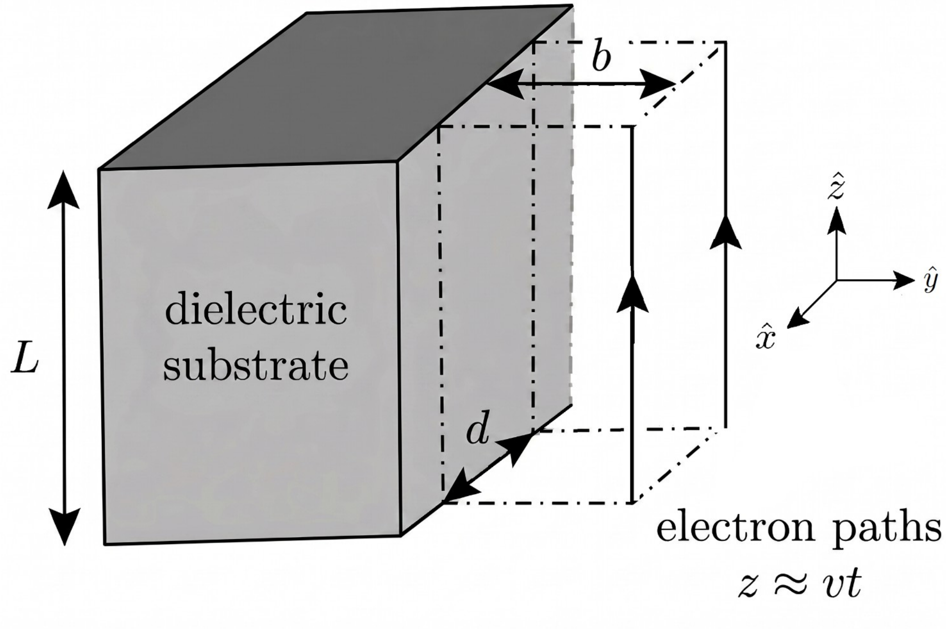

3D Version of the Interaction Model

- If paths are equally weighted, we can use symmetry conditions—e.g., $\psi_{\mathrm{R}}(\mathbf{x}_\perp) = \psi_{\mathrm{L}}^*(\mathbf{x}_\perp) = \psi_0(\mathbf{x}_\perp)$
- Such symmetry conditions allow us to reduce

$$P_e(\mathbf{x}_\perp) = |\psi_0(\mathbf{x}_\perp)|^2 + \mathrm{Re}\left\{ (\psi_0(\mathbf{x}_\perp))^2 \left[c_{\mathrm{R}0}^* c_{\mathrm{L}0} + \sum_{\mathbf{k}} c_{\mathrm{R}\mathbf{k}}^* c_{\mathrm{L}\mathbf{k}} \right] \right\}$$

to calculate the visibility via scattering coefficients:

$$\mathcal{V} = 1 - \sum_{\mathbf{k}} |c_{\mathbf{k}}|^2 [1 - \cos(k_x d)].$$

3D Version of the Interaction Model

- If paths are equally weighted, we can use symmetry conditions—e.g., $\psi_{\mathrm{R}}(\mathbf{x}_{\perp}) = \psi_{\mathrm{L}}^{*}(\mathbf{x}_{\perp}) = \psi_{0}(\mathbf{x}_{\perp})$
- Such symmetry conditions allow us to reduce

$\mathcal{V}$

$$P_e(\mathbf{x}_{\perp}) = |\psi_0(\mathbf{x}_{\perp})|^2 + \mathrm{Re}\left\{ (\psi_0(\mathbf{x}_{\perp}))^2 \left[c_{\mathrm{R0}}^{*} c_{\mathrm{L0}} + \sum_{\mathbf{k}} c_{\mathrm{R}\mathbf{k}}^{*} c_{\mathrm{L}\mathbf{k}} \right] \right\}$$

to calculate the visibility via scattering coefficients:

$$\mathcal{V} = 1 - \sum_{\mathbf{k}} |c_{\mathbf{k}}|^2 [1 - \cos(k_x d)].$$

Total scattering probability….weighted

Markovian Approximation

- For quantized surface modes, the calculated scattering probability scales with the length *L*

$$|c_{\mathbf{k}}|^2 = L\,\frac{\mathrm{d}P_{\mathbf{k}}}{\mathrm{d}z}$$

$$\mathcal{V}(L) \approx 1 - L\sum_{\mathbf{k}} \frac{\mathrm{d}P_{\mathbf{k}}}{\mathrm{d}z}\left[1-\cos(k_x d)\right]$$

- Rewriting this as a rate equation,

$$\gamma(b,d) = \sum_{\mathbf{k}} \frac{\mathrm{d}P_{\mathbf{k}}}{\mathrm{d}z}\left[1-\cos(k_x d)\right]$$

$$\frac{\mathrm{d}\mathcal{V}}{\mathrm{d}z} = -\gamma(b,d)\,\mathcal{V}$$

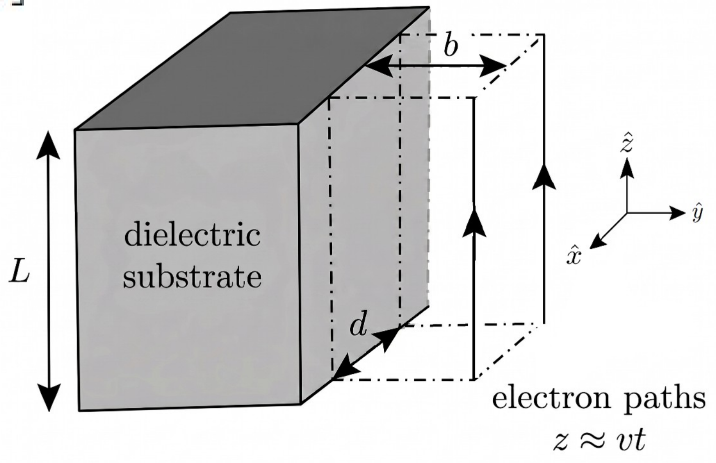

Thermal Weighting

- Now we can help ourselves to the EELS loss-per-mode-per-unit-length models, which lets us extend this ``weighted probability” picture
- If we consider our expressions as rates and include thermal occupations of states, we find that

$$\gamma(b,d,T) = \int_0^\infty \mathrm{d}\omega \int_{-\infty}^{\infty} \mathrm{d}k_x \, \frac{\mathrm{d}^3 P}{\mathrm{d}\omega \, \mathrm{d}k_x \, \mathrm{d}z} \left[1-\cos(k_x d)\right] \coth\left(\frac{\hbar\omega}{2k_B T}\right)$$

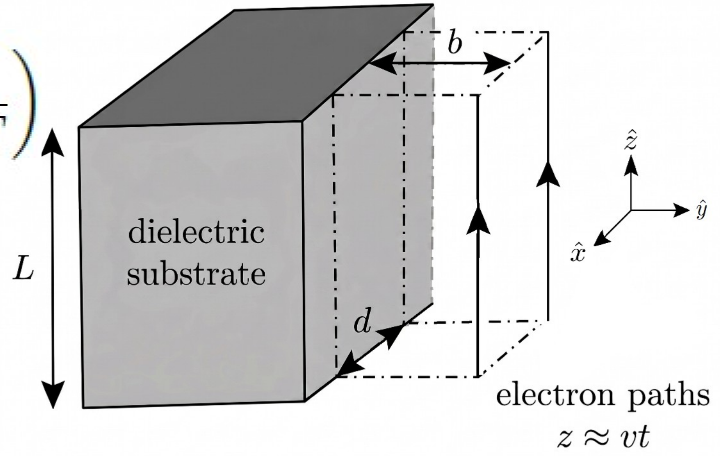

with the visibility evolving as

$$\mathcal{V} = \exp\left[-\gamma(b,d,T)L\right]$$

Elements of "Weighted EELS" Model

$$\gamma(b, d, T) = \int_0^\infty \mathrm{d}\omega \int_{-\infty}^{\infty} \mathrm{d}k_x \, \frac{\mathrm{d}^3 P}{\mathrm{d}\omega \, \mathrm{d}k_x \, \mathrm{d}z} \left[1 - \cos(k_x d)\right] \coth\left(\frac{\hbar\omega}{2k_B T}\right)$$

- This decomposition allows us to clearly see where *b*, *d*, and *T* each contribute

$$\mathcal{V} = \exp\left[-\gamma(b, d, T) L\right]$$

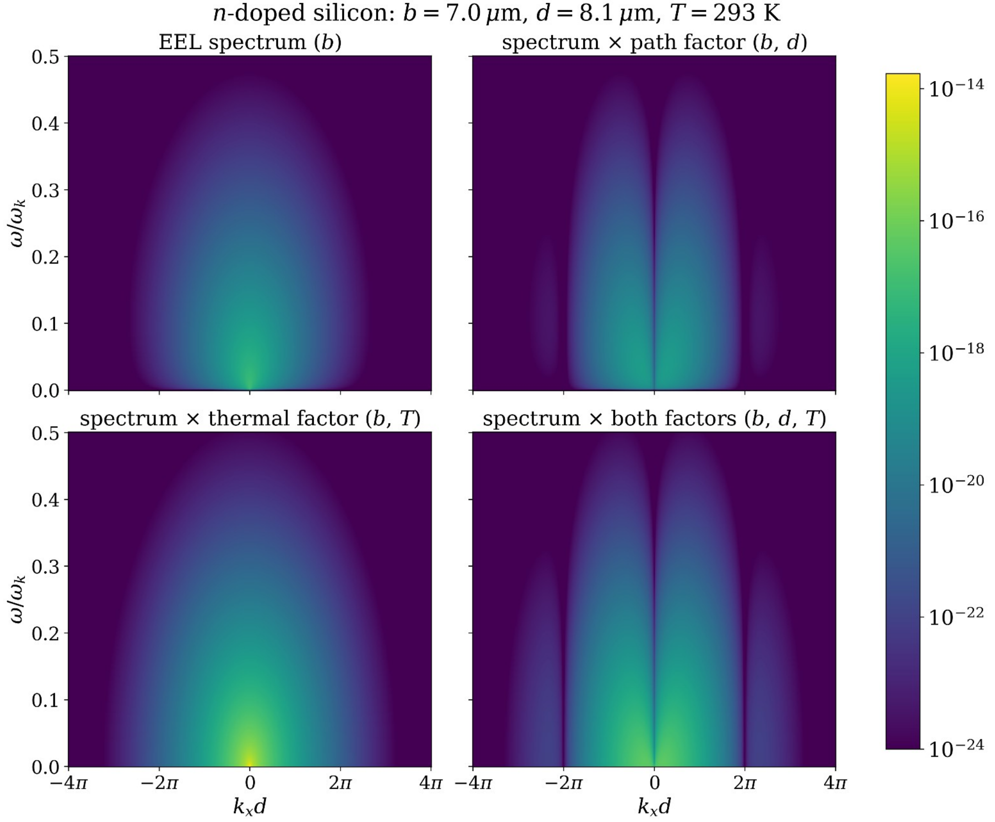

Weighted EELS = "Scheel-Markov"

- We can use electrodynamic EELS loss models in this

$$\gamma(b,d,T) = \int_0^\infty \mathrm{d}\omega \int_{-\infty}^{\infty} \mathrm{d}k_x \, \frac{\mathrm{d}^3 P}{\mathrm{d}\omega\, \mathrm{d}k_x\, \mathrm{d}z} \left[1-\cos(k_x d)\right] \coth\left(\frac{\hbar\omega}{2k_B T}\right)$$

- Doing so exactly recovers "Scheel-Markov" model!

$$\mathcal{V} = \exp\left[-\gamma(b,d,T)L\right]$$

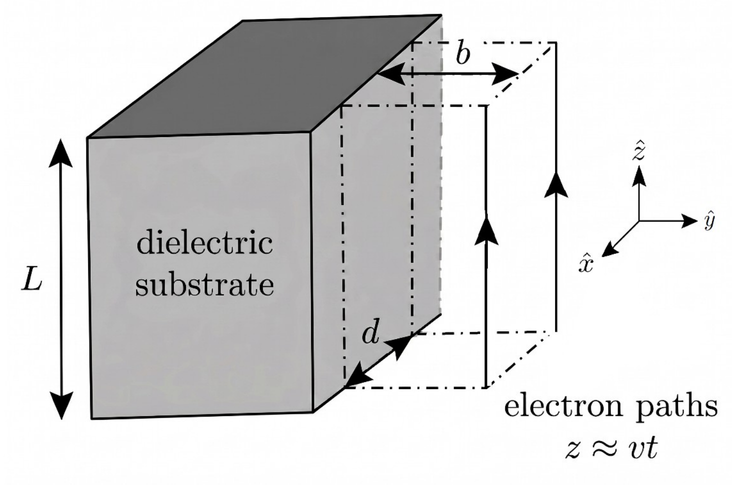

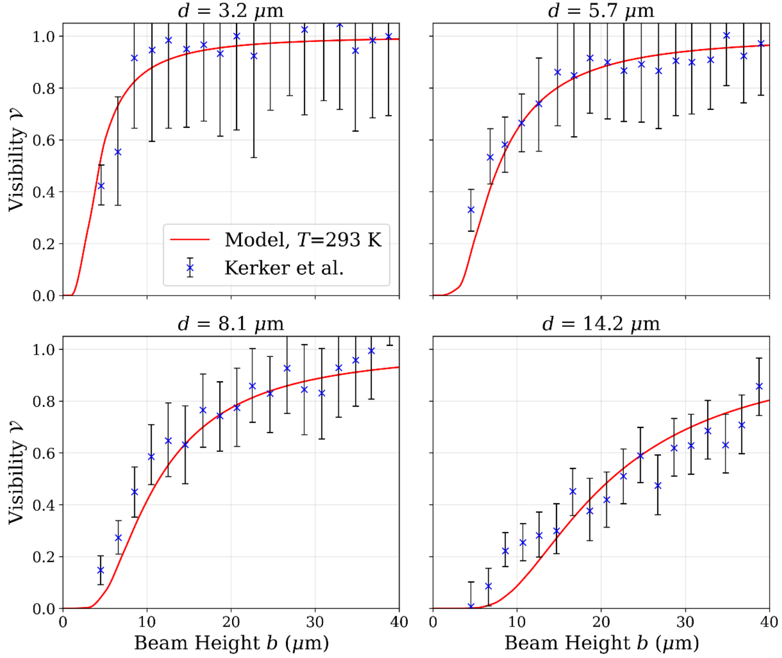

Identifying Contributions

- We can also use less sophisticated EELS loss models

$$\gamma(b,d,T) = \int_0^\infty \mathrm{d}\omega \int_{-\infty}^{\infty} \mathrm{d}k_x \, \frac{\mathrm{d}^3 P}{\mathrm{d}\omega\,\mathrm{d}k_x\,\mathrm{d}z} \left[1-\cos(k_x d)\right] \coth\left(\frac{\hbar\omega}{2k_B T}\right)$$

- This lets us isolate contributions to observations

$$\mathcal{V} = \exp\left[-\gamma(b,d,T)L\right]$$

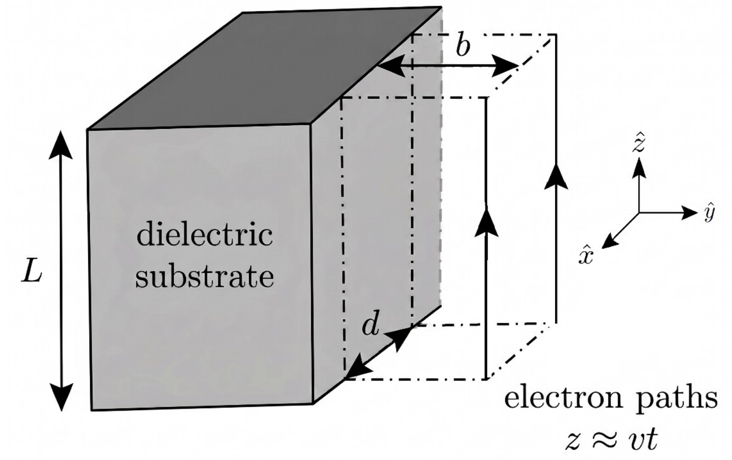

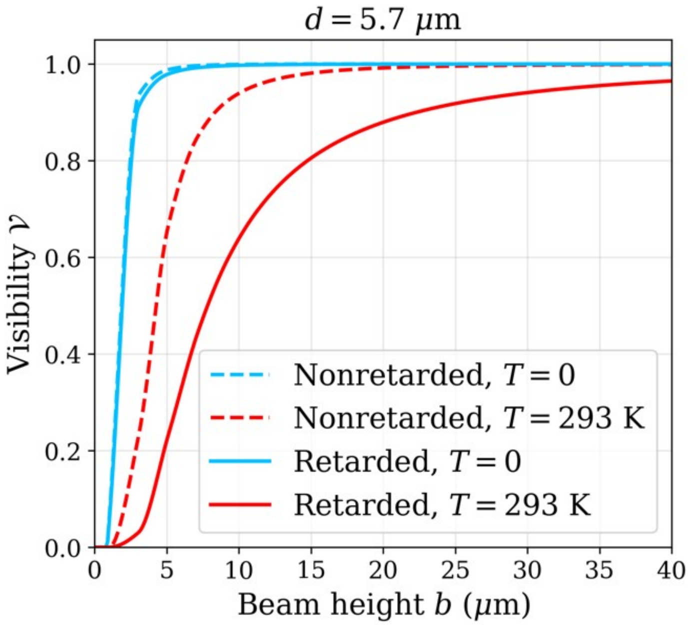

Future Experiments

- This model also lets us think how *V* varies with *T*

$$\gamma(b,d,T) = \int_0^\infty \mathrm{d}\omega \int_{-\infty}^{\infty} \mathrm{d}k_x \, \frac{\mathrm{d}^3 P}{\mathrm{d}\omega\,\mathrm{d}k_x\,\mathrm{d}z} \left[1 - \cos(k_x d)\right] \coth\left(\frac{\hbar\omega}{2k_B T}\right)$$

- C. I. Velasco and collaborators have studied this, and have suggested fringe visibility as a thermal probe

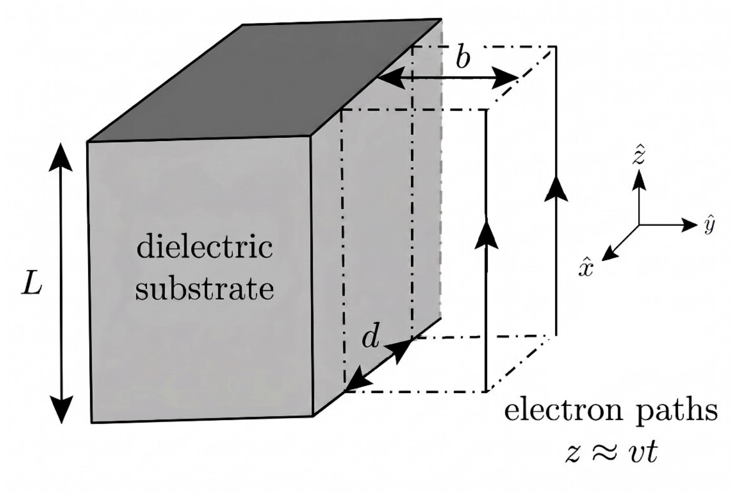

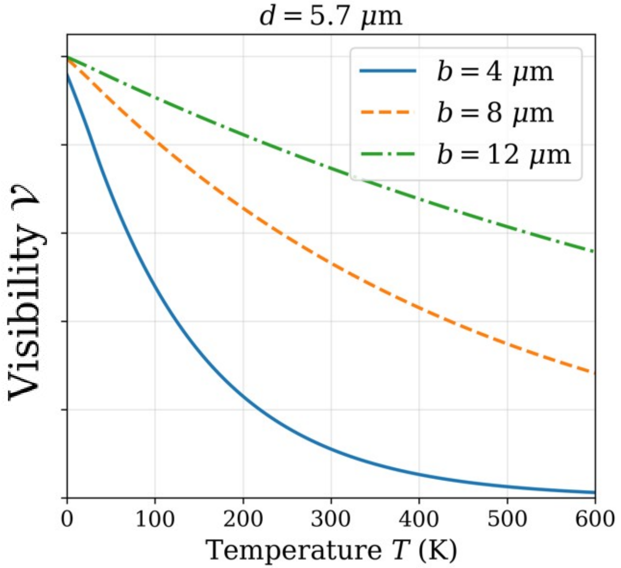

Conclusion

- Decoherence is governed by EELS of surface modes
- Path-distinguishability and temperature factors weight the EEL spectrum
- Thermal dependence of fringe visibility should be experimentally observable

Surface Excitations, Energy Loss, and Decoherence in Electron Interferometry

David Kordahl

arXiv:2606.01004v2